

# Coherent negative mobility of ultracold atoms in an optical lattice

Tobias Salger<sup>1</sup>, Sebastian Kling<sup>1</sup>, Sergey Denisov<sup>2</sup>,  
Alexey V. Ponomarev<sup>2</sup>, Peter Hänggi<sup>2</sup>, and Martin Weitz<sup>1</sup>

<sup>1</sup>*Institut für Angewandte Physik der Universität Bonn,  
Wegelerstrasse 8, 53115 Bonn, Germany*

<sup>2</sup>*Institute of Physics, University of Augsburg,  
Universitätstrasse 1, 86159 Augsburg, Germany*

(Dated: February 24, 2012)

The paradoxical response, when a system produces an output – current, flux or rotation – in the direction opposite to an applied bias or torque, seemingly contradicts Newton’s second law. Nevertheless, such a response, termed absolute negative mobility [1–6], can occur in a system driven far out of thermal equilibrium. In earlier works, the presence of strong decoherence mechanisms was regarded as a prerequisite for negative mobility to appear [2, 7]. Here we report an experimental and theoretical study showing absolute negative mobility in a fully coherent quantum regime. Using a rubidium Bose-Einstein condensate loaded in a time-periodically modulated optical lattice, we observe a negative response from a coherent quantum system. The experimental results are explained in terms of eigenstates of a time-periodic Hamiltonian. Our findings open new possibilities for the control of quantum transport in the decoherence-free limit.

Achieving control of the dynamics of quantum systems is one of the primary goals in the field of nanoscience [8]. While the quest for control of nano- and microscopic systems is usually pursued using static confining potentials, the use of time-dependent potentials is less explored. Ultracold atoms provide attractive model systems for the application of tunable potentials [9], and experiments with atoms in time-dependent optical potentials have demonstrated a variety of possibilities to control atom dynamics [10–13].

Modulated confinements also offer an entirely new perspective, allowing one to focus on the properties of non-equilibrium quantum systems. It is known that not only system characteristics, but also the system response to an external perturbation can drastically differ from those exhibited by the same system near equilibrium [14]. A counterintuitive negative response, namely that a system reacts in the direction opposite to the direction of applied force, may appear due to the interplay of three key factors. These are (i) nonequilibrium conditions, (ii) a nonlinearity, realized, for example, with spatially periodic potentials, and, as it has been reckoned to date, (iii) the presence of decoherence mechanisms [2, 7]. For instance, regimes of absolute negative mobility (ANM) have been detected in solid-state electronic devices [1–3], and have also been investigated theoretically with different classical stochastic models [4, 5]. Recently, absolute negative mobility effects have been observed *in situ*, by tracking an ensemble of charged polystyrene beads with a real-time video microscope [6].

Here we show that a fully coherent single-particle quantum dynamics can exhibit negative

response, which persists on experimentally relevant timescales. We present a theoretical analysis via the Floquet formalism [15] and outline the mechanisms which give rise to ANM quantum regimes. The theoretical predictions are corroborated with the experimental results obtained by measuring the velocity of dilute rubidium atomic BEC loaded into a time-modulated periodic optical potential and subjected to a net bias.

To start, consider the model of a single particle of mass  $M$  placed into a time- and spatially periodic potential,  $V(x)A(t)$  with  $V(x+L) = V(x)$ ,  $A(t+T) = A(t)$ , of periods  $L$  and  $T$  respectively. In addition, assume that the particle is exposed to a tunable net bias,  $F$ . The corresponding Hamiltonian reads

$$H(x, p, t) = p^2/2M + V(x)A(t) + Fx. \quad (1)$$

The undriven system obeys  $A(t) \equiv 1$  and  $F = 0$ ; the Hamiltonian then is spatially-periodic, and the system quasimomentum space is spanned by the Bloch bands,  $E_n(\kappa)$ ,  $\kappa \in [-\pi/L, \pi/L]$  and  $n = 1, 2, \dots$ . By assuming that the initial state is well-localized at the point  $\kappa = 0$ , and considering a weak bias  $F$  as a force which pulls the system through the quasimomentum space, we arrive at a linear time-dependence of the quasimomentum  $\kappa(t) = Ft/\hbar$ . The response of the system to a weak bias on a time scale  $t < 2\pi\hbar/FL = T_B$ , where  $T_B$  is the period of Bloch oscillations, is determined by the curvatures of the bands,  $\hbar^{-2}\partial^2 E_n(k)/\partial\kappa^2$ , i. e. by the effective mass. Hence a negative mobility, following the recipe given by Krömer [16], demands a negative effective mass. This implies that an ANM response from the ground state of a one-dimensional lattice is rendered impossible, because the curvature is always positive near the center of the first Brillouin zone, see Fig. 1a.

The dynamics of time-modulated systems is more diverse. The system Hamiltonian is periodic in time, and the solution of the corresponding Schrödinger equation for a given  $\kappa$  can be obtained as a set of eigenfunctions,  $|\psi_{n,\kappa}(t)\rangle$ . The eigenfunctions satisfy the Floquet theorem, so that  $|\psi_{n,\kappa}(t)\rangle = \exp(-i\epsilon_n(\kappa)t/\hbar) |\phi_{n,\kappa}(0)\rangle$ , where  $|\phi_{n,\kappa}(t+T)\rangle = |\phi_{n,\kappa}(t)\rangle$ . The quasienergies  $\epsilon_n(\kappa)$  are conventionally restricted to the interval  $[-\hbar\pi/T, \hbar\pi/T]$ . The right upper part of Fig. 1b depicts a typical Floquet band structure of a driven optical lattice. It exhibits a complex, web-like structure, which is much more tangled than the Bloch band structure of the undriven system. The set of Floquet states can be ordered in different ways. In the present context it is advantageous to order them with respect to their mean energy at the point  $\kappa = 0$ ,  $\bar{E}_n = \langle\langle\phi_{n,0}|H|\phi_{n,0}\rangle\rangle_T$  [15]. The Floquet bands are well separated,

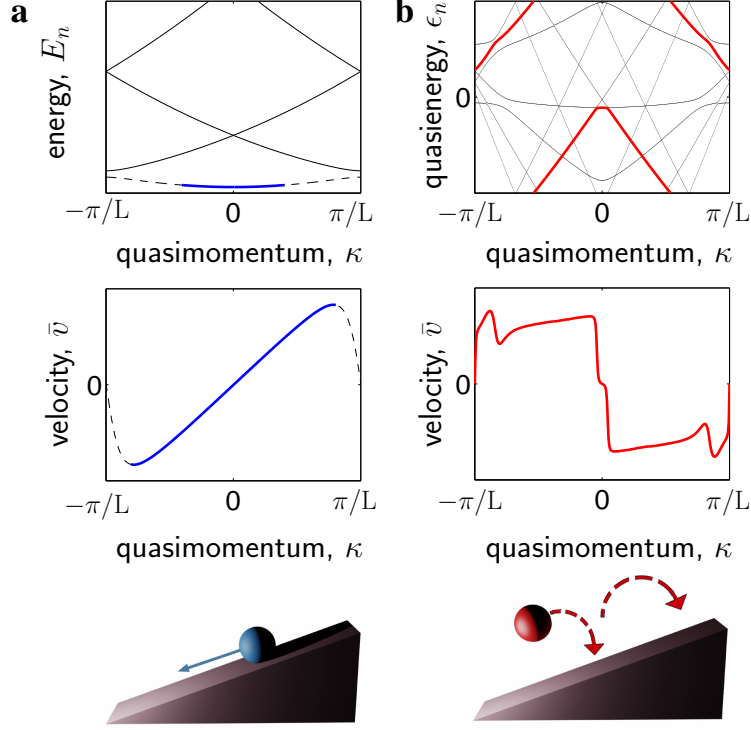


FIG. 1: **Responses to a weak bias of a quantum particle placed into an undriven and ac-driven periodic potentials.** (a) Typical Bloch band structure of an undriven system, with the ground state marked by a dashed line. The action of a weak bias can be represented as a slow motion through the quasimomentum space. The velocity of a particle localized at a certain point in the quasimomentum space is proportional to the slope of the band at the localization point. A particle, initially located in the ground state at the point  $\kappa = 0$ , is capable of producing a weak positive response only. Like a ball placed on a hillside, it always rolls downhill. (b) The Floquet spectrum of the driven system. The average velocity is proportional to the local slope of the corresponding quasienergy band. The thick red line marks a ballistic diabatic band, which is the state of lowest mean energy at the point  $\kappa = 0$ . A quantum particle, initially prepared in this state, produces a strong negative response when subjected to a weak bias, i.e. its center of mass moves into the direction opposite to the applied bias. This effect can be thought as the uphill motion of a bouncing ball.

and, although they may approach each other at the points of avoided crossing [17, 19], their order is preserved over the entire Brillouin zone. An adiabatically slow motion through the quasimomentum space typically respects all avoided crossings. However, for any finite

force,  $F$ , there exists always a set of narrow avoided crossings such that the system ignores them when moving across. The corresponding trajectories in  $\kappa$ -space form so-called diabatic bands [17]. Once populated, a diabatic state would remain decoupled from other Floquet states during the excursion through the quasimomentum space.

The transport properties of Floquet states are characterized by their average velocities,  $\bar{v}_n(\kappa) = \langle v_{n,\kappa}(t) \rangle_T$ , which can be calculated from the corresponding quasienergy,  $\bar{v}_n(\kappa) = \hbar^{-1} \partial \epsilon_n(\kappa) / \partial \kappa$  [18]. When the system Hamiltonian is invariant under time reversal,  $t \rightarrow -t$ , all Floquet bands are flat at the center of the Brillouin zone, thus assuming zero average velocities [19]. Outside the point  $\kappa = 0$  the situation is different: Even in the case when the time-reversal symmetry is present, the Floquet states acquire nonzero velocities upon departure from the center, and some of them form ballistic diabatic bands.

Consider next the situation when at time  $t = 0$  one starts an experiment with a dilute cloud of ultracold atoms, smeared over many wells of an optical potential. An initial wave function in form of a wave-packet localized at the point  $\kappa = 0$  will overlap predominantly with the Floquet ground state of a driven lattice, i. e., with the Floquet state with lowest energy,  $\bar{E}_1$ . Different from the Bloch ground state, the Floquet ground state may itself represent a ballistic diabatic band outside the center of the Brillouin zone, a situation shown in Fig. 1b. Alternatively, a Floquet ground state can be set in contact with one of the ballistic bands, through an avoided crossing at the vicinity of  $\kappa = 0$ . Then, the corresponding ballistic band will also be populated, and will determine the system mobility response, provided that the band was populated substantially and (or) the band velocity is large enough. If, in addition, the band velocity is negative, one will obtain an ANM response.

A general recipe to observe an ANM response is the following: Firstly, the system must be in a deep quantum regime, ideally with only a few Floquet states within the potential range. Otherwise, the atomic cloud would be distributed among many eigenstates, and the system response will consist of many uncorrelated contributions. Secondly, the modulation frequency  $\omega$  should be close to the resonance frequency,  $\omega_R = 4\pi^2 \hbar / L^2 M$ . The resonance modulation will drive the system deeply into a nonequilibrium regime, where the structure of the Floquet spectrum is maximally tangled [17, 19]. The frequency region around the resonance frequency  $\omega_R$  should then be explored systematically in order to locate ANM regions. There is a tip-off that helps in this search. Namely, once one encounters a strong positive response, one can be confident that there is a strong negative response located

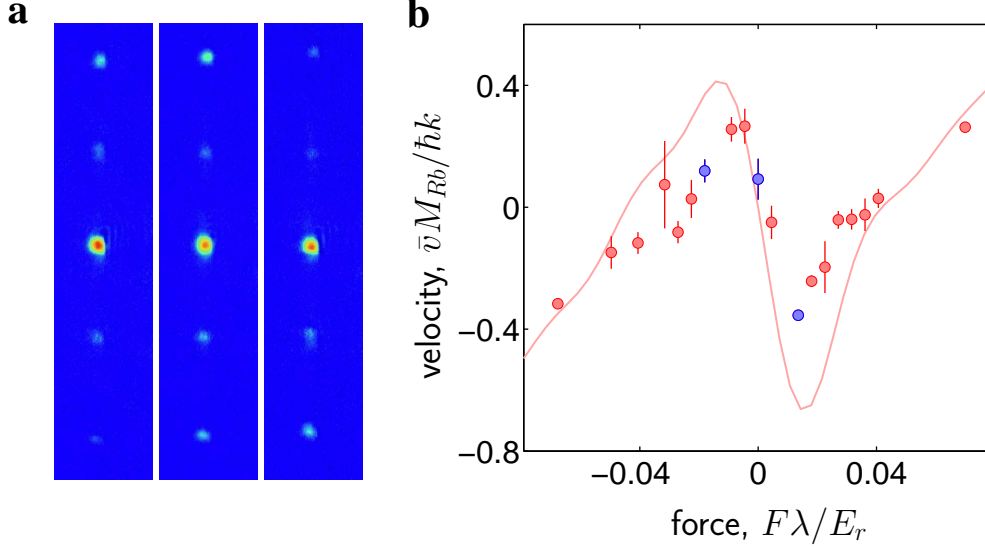


FIG. 2: **Negative mobility of rubidium atoms.** (a) Time of flight images showing the atomic momentum distributions after  $t = 26T$  periods of modulation for  $F = -0.0181 E_r/\lambda$  (left) and  $F = 0.0181 E_r/\lambda$  (right), which is near the maximal observed ANM response respectively, and in the absence of a bias force (center). The used modulation frequency is  $\omega/\omega_R = 1.030$ . The visible atomic diffraction orders are  $s = -2, \dots, 2$  (from bottom to top). (b) Measured mean velocity of the atomic cloud, in units of  $\hbar k/M_{Rb}$ , versus applied force  $F$ , in units of  $E_r/\lambda$ . The error bars show the standard deviation of the mean. The blue data points correspond to the data shown in (a). The solid lines depict the results of a numerical simulation of the experiment for an initial state in the form of a narrow Gaussian packet in the quasimomentum space, with the center at  $\kappa = 0$  and width of  $\sigma_\kappa = 0.04\hbar k$ .

nearby. This is so because the ballistic states with opposite velocities are always paired in systems obeying time-reversal invariance.

In our experiments we use a time-modulated optical potential,  $U(x, t) = V(x)A(t)$ ,

$$V(x) = V_1/2 \cos(2kx) + V_2/2 \sin(4kx), \quad (2)$$

$$A(t) = A_1 \sin^2(\omega t/2) + A_2 \cos^2(\omega t), \quad (3)$$

where  $\lambda$  is the wavelength of the driving laser field and  $k = 2\pi/\lambda$ . With the spatial periodicity  $L = \lambda/2$ , we arrive at a resonance frequency of  $\omega_R = 8\omega_r$ , where  $\omega_r = \hbar k^2/2M_{Rb}$  is the recoil frequency. For the used  $^{87}\text{Rb}$  atoms and  $\lambda = 783\text{nm}$ , we have  $\omega_r = 2\pi \cdot 3.71\text{kHz}$ . The parameters used in experiments are:  $V_1 = 3.1E_r$ ,  $V_2 = 0.7E_r$ , where  $E_r = \hbar\omega_r$  is the recoil

energy, and  $A_1 = 0.7$ ,  $A_2 = 0.44$ . Compared to a standing wave lattice, our biharmonic lattice provides an enhanced control of the system dynamics, while leaving the system perfectly time-symmetric. A rubidium Bose-Einstein condensate is initially freely expanded for  $2.5ms$ , after which its interaction energy has transformed into kinetic energy. Subsequent velocity selection reduces the momentum spread to a value of  $\pm 0.1\hbar k$ , and the ballistically falling atoms are exposed to a temporally varying optical lattice potential with an additional bias force. During the free fall of the atoms, one of the lattice beams is acousto-optically de-tuned with a constant chirp-rate to accelerate the lattice with respect to the lab frame [20]. In this way, we can accelerate the lattice to leave it stationary with the ballistically downwards falling atoms, or leave a variable residual acceleration that acts like an external force. After the interaction with the driven lattice potential of variable net bias, the atoms freely expand for  $15ms$ , and an absorption image is recorded. With this time-of-flight technique, the atomic velocity distribution is analyzed.

Typical experimental data, as presented in Fig. 2a, consist of several atomic diffraction peaks. The mean velocity of the atomic cloud is calculated as  $\bar{v} = \bar{p}/M_{Rb}$  with  $\bar{p} = 2\hbar k \sum_s s |c_s|^2$ , where  $|c_s|^2$  denotes the fraction of atoms in the  $s$ -th order momentum state,  $|2s\hbar k\rangle$ , with  $s = \pm 1, \pm 2$ . The parameters used here were a modulation frequency  $\omega = 1.03\omega_R$ , an interaction time corresponding to  $t = 26T$  periods of the modulation and a net acceleration of  $F = -0.4, 0$ , and  $0.4M_{Rb} \cdot m/s^2$ , which correspond to the dimensionless values  $F\lambda/E_r = -0.0181, 0$  and  $0.0181$  for the left, middle, and right image of Fig. 2a respectively. The measured mean velocity of the atomic cloud versus the external force  $F$  in units of  $E_r/\lambda$  is shown in Fig. 2b. For small values of  $F$ , negative atomic mobility, corresponding to a motion against the external force, is clearly visible. The two data points marked in blue correspond to the data with  $F = \pm 0.0181 E_r/\lambda$ , see the diffraction data of Fig. 2a, left and right, respectively. In other measurements, we have studied the atomic transport versus the drive frequency  $\omega$  at fixed external force. Corresponding data is shown in Fig. 3a for  $F = -0.0181 E_r/\lambda$ , where absolute negative atomic mobility is observed for values of  $\omega/\omega_R$  roughly between 1.02 and 1.15. For smaller frequencies a strongly positive mobility is observed, in accordance with the theoretical prediction that ballistic bands always occur in pairs.

An important issue is the stability of the ANM response. In this respect, it is noteworthy to confront the phenomenon at two different limits, classical and quantum ones. In the

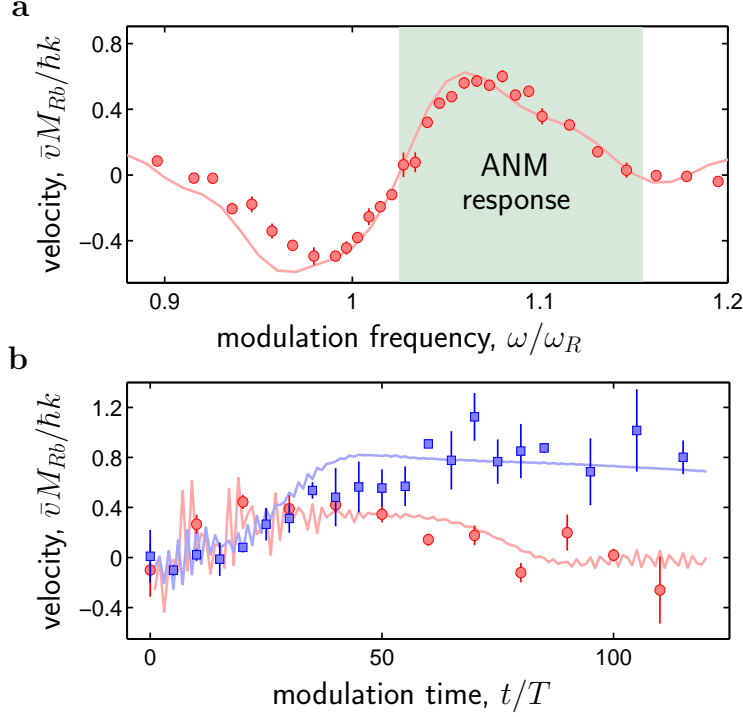


FIG. 3: **Control of mobility.** (a) Mean atomic velocity as a function of the modulation frequency  $\omega$  for a fixed bias force,  $F = -0.0181 E_r/\lambda$ , and exposition time  $26T$ . (b) Time evolution of the mean velocity for two frequencies of the driving,  $\omega/\omega_R = 1.05$  (red dots) and  $\omega/\omega_R = 1.076$  (blue squares). The solid lines depict the results of a numerical simulation of the experiment for an initial state in the form of a narrow Gaussian packet in the quasimomentum space, with the center at  $\kappa = 0$  and width of  $\sigma_\kappa = 0.04\hbar k$ .

classical dissipationless limit, a stationary motion against constant bias is possible [21] due to the existence of invariant manifolds, i.e. transporting regular islands, periodic orbits, and cantori, in the phase space of an ac-driven Hamiltonian system [22]. Diabatic bands can be viewed as the quantum counterpart of classical ballistic manifolds. However, this analogy is not exact. In contrast to classical manifolds, diabatic bands are not completely isolated, since any finite bias sets the band into contact with other states. All avoided crossings have finite widths, and the Landau-Zener tunneling between Floquet states [15] will eventually lead to the regime of acceleration along the applied bias. Nevertheless, the relaxation to this asymptotic regime can be extremely slow, thus transforming the negative response into a long-lasting metastable phenomenon. In order to confirm this prediction, we measured the velocity of the atomic cloud as a function of the exposition time for two different values



of the driving frequency. Fig. 3b presents corresponding results of the measurements. For a modulation frequency  $\omega/\omega_R = 1.05$  (red dots), the mean momentum of the atomic cloud increases initially, reaching a broad maximum value of  $0.4\hbar k$  after around 30 modulation periods, and then starts to decrease again, approaching zero at  $t \approx 80T$ . When slightly changing the modulation frequency to  $\omega/\omega_R = 1.076$  (blue squares), the observed atomic momentum increases to roughly  $0.9\hbar k$ , with this value of the atomic transport being maintained to much longer modulation times. This finding is in agreement with the fact that the structure of Floquet bands is very sensitive to the system parameters, and the atomic response can be controlled over a wide range.

Our results can be interpreted as a realization of a quantum engine [23], in which the system self-adjusts itself to perform a work against an external force. The observed quantum ANM effect can not only be seen as a next step towards fully controllable transport of ultracold matter [24, 25], but also highlights the salient fact that single-particle quantum systems can produce a spectrum of nontrivial phenomena, when moved far from equilibrium. For the future, we expect that inclusion of many-body effects of interacting condensate atoms [9, 26] will enrich the present spectrum even further.

This work was supported by the DFG Grants We1748/7 (M.W.), HA1517/31-2 (S.D. and P.H), the German Excellence Initiative “Nanosystems Initiative Munich (NIM)” (A.V.P., S.D. and P.H.).

## Supplementary Material

**Experimental set-up and procedure.** The experimental set-up was described previously in Refs. [13, 20]. A spin-polarized Bose-Einstein condensate with about  $6 \cdot 10^4$   $^{87}\text{Rb}$  atoms in the Zeeman sublevel  $m_F = 0$  is created by evaporative cooling in a quasistatic dipole trap with an applied small magnetic quadrupole field. The dipole trap is then switched off and the cloud performs a ballistic free fall in the earth’s gravity field for  $2.5\text{ms}$ , where interaction energy is transformed into kinetic energy. The condensate is then exposed to a  $350\text{ }\mu\text{s}$ -long Bragg pulse, which transfers a narrow slice of atoms with momentum spread  $\pm 0.1\hbar k$  into a momentum state  $|2\hbar k\rangle$ , followed by a  $150\text{ }\mu\text{s}$ -long Raman pulse transferring the momentum-reduced sample into the zero momentum state  $|0\hbar k\rangle$  with  $m_F = -1$ . The velocity selected atoms are subsequently subjected into a vertical Fourier-synthesized optical

lattice potential that is periodically modulated in time. The lattice potential is generated by superimposing two lattice harmonics with spatial periodicities  $\lambda/2$  and  $\lambda/4$ , with the latter being generated by a multiphoton Raman technique [20]. Here  $\lambda = 783nm$  is the laser wavelength, some  $3nm$  red-detuned from the rubidium  $D2$ -line. The experiments are done in ballistic free fall with the gravity force in the atomic frame partially compensated in a controllable manner by linearly chirping the frequency of one of the laser beams. After a fixed exposition time, all laser fields are switched off and the atoms freely expand for  $15ms$ , after which an absorption image is recorded onto a CCD camera.

**Numerical methods.** We model the dynamics of a wave-packet, initially localized at the center of the Brioullin zone, with a wave function  $|\Psi[\kappa]\rangle = \frac{1}{\sqrt{2\pi}\sigma_\kappa} \int_{-\infty}^{\infty} e^{-\kappa^2/2\sigma_\kappa^2} d\kappa$ . This is a good approximation of a momentum slice used in the experiments, and the dispersion  $\sigma_\kappa$  serves as a fitting parameter. The initial wave-packet has been sampled in a first Brillouin zone with 5000 points. Every slice is then propagated by using the integration scheme from Ref. [19]. Finally, the contribution from all points are summed up. Numerical parameters correspond to the values given in the main text.

- 
- [1] Sturman, B. I. & Fridkin, V. M. *The photovoltaic and photorefractive effects in noncentrosymmetric materials* (Gordon and Breach, Philadelphia, 1992).
  - [2] Keay, B. J. *et al.* *Dynamic localization, absolute negative conductance, and stimulated, multiphoton emission in sequential resonant tunneling semiconductor superlattices*, Phys. Rev. Lett. **75**, 4102 (1995).
  - [3] Nagel, J. *et al.* *Observation of negative absolute resistance in a Josephson junction*, Phys. Rev. Lett. **100**, 217001 (2008).
  - [4] Eichhorn, R., Reimann, P., & Hänggi, P. *Brownian motion exhibiting absolute negative mobility*, Phys. Rev. Lett. **88**, 190601 (2002).
  - [5] Machura, L. *et al.* *Absolute negative mobility induced by thermal equilibrium fluctuations*, Phys. Rev. Lett. **98**, 040601 (2007).
  - [6] Ros, A. *et al.* *Absolute negative particle mobility*, Nature **436**, 928 (2005).
  - [7] Tien, P. K. & Gordon, J. P. *Multiphoton process observed in the interaction of microwave fields with the tunneling between superconductor films*, Phys. Rev. **129**, 647 (1963).

- [8] Di Ventra, M., Evoy, S. James, & Heflin, R. *Introduction to nanoscale science and technology* (Springer, New York, 2004).
- [9] Bloch, I. *Ultracold quantum gases in optical lattices*, Nature Phys. **1**, 23 (2005).
- [10] Madison, K. W. *et al.* *Dynamical Bloch band suppression in an optical lattice*, Phys. Rev. Lett. **81**, 5093 (1998).
- [11] Gemelke, N. *et al.* *Parametric amplification of matter waves in periodically translated optical lattices*, Phys. Rev. Lett. **95**, 170404 (2005).
- [12] Zenesini, A. *et al.* *Coherent control of dressed matter waves*, Phys. Rev. Lett. **102**, 100403 (2009).
- [13] Salger, T. *et al.* *Directed transport of atoms in a Hamiltonian quantum ratchet*, Science **326**, 1241 (2009).
- [14] Baiesi, M., Maes, C., & Wynants, B. *Fluctuations and response of nonequilibrium states*, Phys. Rev. Lett. **103**, 010602 (2009).
- [15] Grifoni, M. & Hänggi, P. *Driven quantum tunneling*, Phys. Rep. **304**, 219 (1998).
- [16] Krömer, H. *Proposed negative-mass microwave amplifier*, Phys. Rev. **109**, 1856 (1958).
- [17] Miyazaki, S. & Kolovsky, A. R. *Quasienergy-band structure of a periodically driven system with translational symmetry*, Phys. Rev. E **50**, 910 (1994).
- [18] Sambe, H. *Steady states and quasienergies of a quantum-mechanical system in an oscillating field*, Phys. Rev. A **7**, 2203 (1973).
- [19] Denisov, S., Morales-Molina, L., Flach S., & Hänggi, P. *Periodically driven quantum ratchets*, Phys. Rev. A **75**, 063424 (2007).
- [20] Salger, T., Geckeler, C., Kling, S., & Weitz, M. *Atomic Landau-Zener tunneling in Fourier-synthesized optical lattices*, Phys. Rev. Lett. **99**, 190405 (2007).
- [21] Denisov, S., Flach, S., & Hänggi, P. *Stationary Hamiltonian transport with dc bias*, Europhys. Lett. **74**, 588 (2006).
- [22] Schanz, H., Dittrich, T., & Ketzmerick R. *Directed chaotic transport in Hamiltonian ratchets*, Phys. Rev. E **71**, 026228 (2005) .
- [23] Hänggi, P. & Marchesoni, F. *Artificial Brownian motors: Controlling transport on the nanoscale*, Rev. Mod. Phys. **81**, 387 (2009).
- [24] Alberti, A., Ivanov, V. V., Tino, G. M., & Ferrari, G. *Engineering the quantum transport of atomic wavefunctions over macroscopic distances*, Nature Phys. **5**, 547 (2009).

- [25] Haller, E. *et al.* *Inducing transport in a dissipation-free lattice with super Bloch oscillations*, Phys. Rev. Lett. **104**, 200403 (2010).
- [26] Ruichao Ma *et al.* *Photon-assisted tunneling in a biased strongly correlated Bose gas*, Phys. Rev. Lett. **107**, 095301 (2011).